Gallic Acid Ameliorates *Aspergillus Fumigatus* Keratitis Through Reducing Fungal Load and Suppressing the Inflammatory Response

Songying Luan,[1] Xudong Peng,[1] Jing Lin,[1] Yingxue Zhang,[2] Lu Zhan,[1] Jiao Yin,[1] Junjie Luan,[1] Xiaoyue Ji,[1] and Guiqiu Zhao[1]

[1]Department of Ophthalmology, The Affiliated Hospital of Qingdao University, Qingdao, Shandong Province, China
[2]Department of Biochemistry, Microbiology and Immunology, Wayne State University School of Medicine, Detroit, Michigan, United States

Correspondence: Guiqiu Zhao and Xudong Peng, Department of Ophthalmology, The Affiliated Hospital of Qingdao University, NO. 16 Jiangsu Road, Qingdao, Shandong Province 26600, China; zhaoguiqiu_good@126.com, drpxd@uw.edu.

Received: September 6, 2021
Accepted: April 25, 2022
Published: November 9, 2022

Citation: Luan S, Peng X, Lin J, et al. Gallic acid ameliorates *aspergillus fumigatus* keratitis through reducing fungal load and suppressing the inflammatory response. *Invest Ophthalmol Vis Sci.* 2022;63(12):12. https://doi.org/10.1167/iovs.63.12.12

Purpose. The purpose of this study was to explore the antifungal and anti-inflammatory effects of gallic acid (GA) on *Aspergillus fumigatus* (*A. fumigatus*) keratitis.

Methods. CCK-8 assay and Draize eye test were used to determine the non-cytotoxic concentration of GA in RAW264.7 cells and an *A. fumigatus* keratitis mouse model. The antifungal effects of GA were analyzed using minimal inhibitory concentration (MIC), biofilm formation test, fungal adherence assay, calcofluor white staining, and propidium iodide staining. The therapeutic effects of GA were estimated by slit lamp photographs, clinical score, hematoxylin and eosin (H&E) staining, and Periodic acid-Schiff staining in vivo. Immunofluorescence staining and myeloperoxidase assay were conducted to identify neutrophil infiltration and activity. RT-PCR, ELISA, and Western blot were performed to detect the expression of pro-inflammatory cytokines and Nrf2/HO-1.

Results. In HCECs and *A. fumigatus* keratitis mouse model, GA at 100 µg/mL did not affect cell viability, thus this concentration was applied to subsequent experiments. In vitro, GA significantly inhibited *A. fumigatus* growth, biofilm formation, and adhesion. In vivo, 100 µg/mL GA alleviated the severity of fungal keratitis (FK) by repressing fungal load, reducing neutrophil infiltration, and lowering MPO activity. Besides, the expression of IL-1β, TNF-α, LOX-1, and COX-2 was inhibited, whereas Nrf2 and HO-1 expression was enhanced at both mRNA and protein levels in the 100 µg/mL GA treated group in comparison to PBS control.

Conclusions. GA ameliorates FK severity through inhibiting *A. fumigatus* load, reducing neutrophils infiltration, downregulating the expression of pro-inflammatory cytokines, and enhancing the Nrf2/HO-1 pathway, which provides new insight into *A. fumigatus* keratitis treatment.

Keywords: gallic acid (GA), fungal keratitis (FK), antifungal, anti-inflammatory, Nrf2/HO-1

Fungal keratitis (FK) is an intractable ocular infection that can result in a corneal ulcer, perforation, and even blindness,[1] which attribute to not only the presence of fungal hyphae, but also severe inflammatory response.[2] The incidence of FK ranges from 6% to 56% in various regions of the world,[3] suggesting the need to explore effective antifungal and anti-inflammatory agents.

FK is commonly caused by *A. fumigatus*, *Aspergillus flavus* (*A. flavus*), and *Fusarium*.[1] Over the past 10 years, *A. fumigatus* has become the most prevalent airborne fungal pathogen, causing severe and usually fatal invasive infections in immunocompromised hosts in developed countries.[4] Due to agricultural ocular trauma, postoperative corneal infection, long-term use of contact antibiotics and lenses, and excessive use of corticosteroids, the incidence of FK has been increasing, especially in developing countries and tropical regions.[1–3] However, current antifungal drugs have significant limitations. For example, in a toxicity evaluation by Foster et al., amphotericin B was found to severely retard the rate of debrided corneal closure and manifested dramatic pathologic changes (evaluated on the bases of scores for quality of regenerating epithelium, stromal edema and haze, and iritis) that worsened each day with the continuation of therapy.[5] Hence, from the abovementioned discussion, local toxicities present an important aspect of the challenge in the ocular application of amphotericin B. The other commonly used antifungal drug is natamycin. But natamycin has poor permeability, which barely passes an intact corneal epithelium due to its molecular mass (666 Da).[6] In support, animal studies showed that the efficacy of natamycin was substantially lessened in intact versus debrided corneas.[7] More importantly, amphotericin B and natamycin are costly, and repeated application in a relatively short period is required to prevent FK re-occurrence and drug resistance.[7] This

therapeutic strategy may reduce follow-up visits, especially those who cannot afford medical care. Therefore, it is urgent to find effective and affordable treatment for FK.

Gallic acid (GA; 3,4,5-trihydroxy benzoic acid) is a natural polyphenol ubiquitously present in fruits, vegetables, legumes, and herbal medicines.[8] Previous studies have reported that GA and its derivatives possess a variety of biological properties, such as antioxidative, antiviral, anticancer, and anti-inflammatory activities.[9] For example, GA can bind and quench reactive oxygen species (ROS) with high affinity, thereby ameliorating oxidative stress-associated tissue damage in many diseases, including cancers, liver diseases, neuroinflammation, and inflammatory bowel disease.[10–13] GA exhibits broad-spectrum antimicrobial activities, including antifungal, antibacterial, and antiviral in vitro.[14] GA significantly inhibited *Trichophyton rubrum* growth by repressing the activity of two key enzymes involved in fungal ergosterol biosynthesis, squalene epoxidase, and sterol 14α-demethylase P450 (CYP51), to interfere with fungal membrane integrity,[15] and the fungicidal efficiency was comparable to fluconazole.[14] Recently, GA extracted from *Cassia fistula* has been shown to have a potent antifungal activity on fluconazole-resistant *Candida* species isolated from patients with HIV,[16] whereas the antifungal mechanisms remain unclear.

On the other hand, corneal inflammation and its associated complications are the leading cause of vision impairment in FK. The excessive inflammatory response induced aggregation of immune cells, such as neutrophils, macrophages, and dendritic cells, further promotes the production of pro-inflammatory cytokines, such as IL-1β, TNF-α, and COX-2, resulting in corneal damage, nubecula, and even corneal perforation.[17] Thus, controlling the excessive immune response in FK is beneficial in preventing inflammation-related corneal injury. In addition to its antifungal property, GA plays an anti-inflammatory role in different animal models and human subjects. For instance, GA attenuated lipopolysaccharides (LPS)-induced neuroinflammation and neurotoxicity in the rat brain and BV-2 microglial cells and significantly reduced IL-1β expression.[18] GA also acts as the gastroprotective property in ethanol-induced gastric ulcer rats via downregulating the serum levels of pro-inflammatory cytokines, including IL-1β and tumor necrosis factor α (TNF-α) and activating nuclear factor-erythroid 2-related factor 2 (Nrf2)/heme oxygenase (HO-1) pathway.[19] However, to date, there is no study investigating the role of GA in FK.

In this study, we demonstrate the antifungal and anti-inflammatory effects of GA in mouse macrophages and an *A. fumigatus* keratitis mouse model. GA treatment could alleviate the severity of *A. fumigatus* keratitis in mice not only by reducing fungal load but also by repressing the expression of pro-inflammatory cytokines and enhancing the Nrf2/HO-1 pathway. Our findings identified the antifungal and anti-inflammatory related mechanisms of GA in *A. fumigatus* keratitis, providing a new alternative for FK treatment.

Materials and Methods

Gallic Acid and Natamycin Preparation

GA powder (CAS 149-91-7; Macklin Biochemical Co. Ltd., Shanghai, China) was dissolved in phosphate-buffered saline (PBS; Solarbio, Beijing, China) at a storage concentration of 10 mg/mL, and further diluted to the required concentrations with Dulbecco's Modified Eagle Medium (DMEM; Solarbio) for RAW264.7 cells and human corneal epithelial cells (HCECs), and Sabouraud liquid medium which contains protein, agar, and glucose for fungal conidia treatment.

Natamycin (NAT) powder (CAS 7681-93-8; Macklin Biochemical Co. Ltd., Shanghai, China) was dissolved in PBS (Solarbio) at a storage concentration of 8 mg/mL, and further diluted to the required concentrations with DMEM (Solarbio) for RAW264.7 cells, and Sabouraud liquid medium for fungal conidia treatment.

Aspergillus Fumigatus Culture

A. fumigatus standard strain 3.0772 was obtained from China General Microbiological Culture Collection Center (Beijing, China), and stored in the refrigerator at −80°C. Its aerobic and culture temperature was 25 to 28°C. The second generation of *A. fumigatus* was inoculated in 150 mL Erlenmeyer flasks containing Sabouraud liquid medium. After 48 hours of shaking at 120 rpm, 37°C, the hyphae were washed using sterile PBS 3 times and collected by centrifugation at 5000 rpm for 15 minutes. The supernatant was discarded, and the hyphae were resuspended by 5 mL DMEM.

For active hyphae preparation, we pipetted 10 µL of diluted fungi into a hemocytometer and counted the number of hyphae under the microscope. According to the counting results, the hyphae solution was then diluted using DMEM to a final concentration of approximately 3×10^8 hyphal fragments/mL. The active *A. fumigatus* hyphae were also inoculated onto Sabouraud agar plates and incubated for 36 to 48 hours at 37°C. Spores were scraped, diluted with PBS, and counted using the same approach as described above. They were adjusted to 3×10^7/mL for minimum inhibitory concentration (MIC), biofilm formation test, fungal adherence assay, calcofluor white staining, and Propidium iodide (PI) staining.

The inactive hyphae were prepared using active hyphae by overnight incubation with 75% alcohol. After being washed by DMEM, the inactive hyphae were diluted and counted using the same approach as described above. The final concentration was also adjusted to 10^8 hyphal fragments /mL.

Cell Culture and *A. fumigatus* Stimulation

RAW264.7 cells (Chinese Academy of Sciences, Shanghai, China) were cultured as described previously.[20] Briefly, RAW264.7 cells were seeded in 6- and 12-well plates for 24 hours until 80% to 90% confluency, then stimulated with inactive hyphae at 3×10^6 hyphal fragments/mL for 1 hour, followed by GA incubation at a final concentration of 100 µg/mL or NAT at 8 µg/mL. RAW264.7 cells were collected at 8 hours for RT-PCR to detect the mRNA levels of IL-1β, TNF-α, LOX-1, and COX-2, and collected at 24 hours for Western blot to examine the protein levels of HO-1 and Nrf2. The supernatant at 24 hours was used for ELISA to estimate the protein levels of IL-1β and TNF-α.

Minimum Inhibitory Concentration

The MIC assay method refers to the standardized microdilution method.[21] GA was diluted using Sabouraud liquid medium by a 2-fold dilution method to 12.5, 25, 50, 100, 200, 400, and 800 µg/mL in a sterile Eppendorf tube, and *A. fumigatus* spores at 3×10^5/mL were added to each

tube. After being mixed adequately, each solution was transferred into a 96-well plate (100 µL/well) with 6 repetitions for each concentration. After 48 hours of incubation at 37°C, the optical density (OD) was measured at 540 nm with a microplate reader. Two control conditions (GA-free medium with or without conidium) were simultaneously set up for each plate.

Cell Counting Kit-8 Assay

Human corneal epithelial cells (HCECs; PCS-700-010; kindly provided by the Ocular Surface Laboratory Zhongshan Ophthalmic Center, China) were cultured using the previous method.[22] HCECs (3×10^4/mL) were suspended and transferred into 96-well plates with sterile DMEM and incubated for 24 hours until 90% confluency. After being rinsed with sterile PBS, each well was incubated with 100 µL different concentrations of GA diluted with DMEM for 48 hours, followed by a 2-hour incubation with 10 µL CCK-8 (MedChemExpress) at 37°C. Then, OD at 450 nm was measured by a microplate reader.

Draize Eye Test

To evaluate the ocular toxicity of GA in mouse models, a Draize eye test was performed as described previously.[23] Briefly, the left eyes of the mice were treated with 5 µL of GA (10^4 and 100 µg/mL), and the right eyes were treated with PBS 3 times a day as a control. At 1, 3, and 5 days post-treatment, 1 µL of 1% luciferin sodium (Meilunbio, Dalian, China) was dropped into the conjunctival sac of each mouse, and corneal fluorescein staining was examined by slit-lamp microscopy under cobalt blue light ($n = 5$/group/time). Corneal fluorescein staining (CFS) scores were evaluated according to the Organization for Economic and Cooperative Development (OECD) grading scale, which involved weighting and summing six components of directly observable changes in the eye's anterior segment, including the density and area of corneal opacification, the severity of iritis, conjunctival redness, edema, and discharge.

Biofilm Formation

A colorimetric microtiter plate assay was performed to determine the biofilm-forming capacity of *A. fumigatus* exposed to different concentrations of GA.[23] Conidia suspension (3×10^5/mL) was transferred into a 24-well plate with 1000 µL per well and incubated for 48 hours at 37°C. After biofilm formed, wells were gently decanted and rinsed with sterilized PBS. Then, 1000 µL Sabouraud medium containing GA (0, 12.5, 25, 50, 100, and 200 µg/mL) was added to each well in triplicate and incubated for 48 hours at 37°C. After air drying, biofilms were fixed with glutaraldehyde and stained with 100 µL per well of 1% crystal violet (Solarbio) for 15 minutes. Unbound dye was washed off with PBS. After air drying, dye bound to biofilm was released with 100 µL of 95% ethanol per well without shaking. The OD of each well was measured at 620 nm using a microplate reader.

Calcofluor White Staining

Calcofluor white staining was conducted to determine the cell wall integrity of *A. fumigatus*. GA was diluted in different concentrations (0, 50, 100, and 200 µg/mL) with a Sabouraud medium and was incubated with *A. fumigatus* conidia (3×10^4/mL) in 6-well plates for 48 hours at 37°C. Then, 1 µg/mL caspofungin acetate (CAS 179463-17-3; Macklin Biochemical Co. Ltd., Shanghai, China) was used for positive control. After decanted supernatant, 500 µL of Calcofluor White Stain (Sigma-Aldrich, USA), a nonspecific fluorochrome that binds to cellulose and chitin of fungi, was added and incubated at room temperature (RT) for 30 minutes. The staining pictures were photographed using the fluorescence microscope (Zeiss Axiovert, Jena, Germany; at 20× magnification).

Propidium Iodide Staining

To examine the cell membrane integrity of *A. fumigatus*, PI staining was performed as previously described.[24] The conidia suspension of *A. fumigatus* (2×10^6 hyphal fragments /mL) was seeded on a 6-well plate and incubated at 37°C for 24 hours. Then, the hyphae were washed, centrifuged (12,000 rpm for 10 minutes), transferred to a new 6-well plate, and then incubated with 0, 50, 100, and 200 µg/mL GA at 37°C for 24 hours. The 8 µg/mL NAT was used as a positive control. After harvesting and washing with sterile PBS, the fungal hyphae were incubated with PI (Leagene Biotechnology, Beijing, China) solution for 15 minutes at RT in the dark. Images were photographed with a fluorescence microscope (Zeiss Axiovert, Jena, Germany; at 20× magnification).

Fungal Adhesion Assay

HCECs were inoculated to the chambered slides (four/slide) and incubated at 37°C until 30% confluency. After being rinsed with sterile PBS, cell chambers were incubated with conidia suspension (3×10^4/mL) for 1 hour and treated with GA at 100 µg/mL for 3 hours at 37°C. Then, the slides were washed with sterile PBS, air-dried, and stained through hematoxylin and eosin (H&E). The number of spores that adhered to the surface of HCECs was counted, averaged, and expressed as the number of adherent spores/cells. All specimens were observed and photographed by optical microscopy (Axio Vert; Zeiss, Jena, Germany; at 400× magnification).

A. Fumigatus Keratitis Mouse Models

Healthy female 8-week-old C57BL/6 mice (SiPeiFu Biotechnology Co. Ltd., Beijing, China) weighed between 20 and 30 grams (g) were treated according to the ARVO Statement regarding the Use of Animals in Ophthalmology and Vision Research. The establishment of the *A. fumigatus* keratitis model was in accordance with Zhan et al.[22] Mice were abdominally anesthetized with 4 mL of 8% chloral hydrate, and each left eye was a blank control. The right corneal stroma was injected with 2.5 µL *A. fumigatus* conidia suspension (3×10^7/mL) with a microsyringe (10 µL; HAMILTON, type #1701) under a slit-lamp microscope (DS126431; Cannon, Japan; at 4× magnification). After 4 hours, 5 µL of GA (100 µg/mL) was dripped on the right eye 3 times a day in the GA-treated groups, and 5 µL of PBS was dripped on the right eye 3 times a day as a control. The 8 µg/mL NAT was used as comparator treatment. Based on the observation under a slit lamp at 1, 3, and 5 days post-infection (p.i.), the severity of keratitis ($n = 8$/group) was evaluated by clinical score referred to the 12-point scoring system.[25] Briefly, each aspect of opacity density, opacity area,

Investigative Ophthalmology & Visual Science

Table. Primer Sequences Used for RT-PCR

Gene	GenBank No.	Primer Sequence (5′-3′)
Mouse *β-actin*	NM_007393.5	F: GAT TAC TGC TCT GGC TCC TAG C R: GAC TCA TCG TAC TCC TGC TTG C
Mouse *IL-1β*	NM_008361.4	F: CGC AGC AGC ACA TCA ACA AGA GC R: TGT CCT CAT CCT GGA AGG TCC ACG
Mouse *TNF-α*	NM_013693.3	F: ACC CTC ACA CTC AGA TCA TCT T R: GGT TGT CTT TGA GAT CCA TGC
Mouse *LOX-1*	NM_138648.2	F: AGG TCC TTG TCC ACA AGA CTG G R: ACG CCC CTG GTC TTA AAG AAT TG
Mouse *COX-2*	NM_011198.3	F: TGC ACT ATG GTT ACA AAA GCT GG R: TCA GGA AGC TCC TTA TTT CCC TT
Mouse *TGF-β*	NM_011577.1	F: AAC AAT TCC TGG CGT TAC CTT R: CTG CCG TAC AAC TCC AGT GA
Mouse *HO-1*	NM_010442.2	F: TGC AGG TGA TGC TGA CAG AGG R: GGG ATG AGC TAG TGC TGAT CTG G
Mouse *Nrf-2*	NM_010902.4	F: GAA GTT CCC GTG AGT CCT GGT C R: CCT CTA AGC GGC TTG AAT GTT TG

and surface regularity scores were 0 to 4 points. A total score of 0 to 5 is a mild infection, 6 to 9 is a moderate infection, and 10 to 12 is a severe infection. The corneas at 3 and 5 days p.i. were harvested for RT-PCR. The corneas at 3 days p.i. were removed for myeloperoxidase (MPO). The mouse eyeballs at 3 days p.i. were removed for H&E staining, PAS staining, and immunofluorescence staining (IFS).

Myeloperoxidase Assay

Mice corneas at 3 days p.i. (n = 5/group) were harvested and homogenized, then followed with the instruction of the MPO test kit (Nanjing Jiancheng Bioengineering Institute, Nanjing, China). MPO was measured spectrophotometrically at 460 nm at 37°C. The line slope was related to the MPO activity (unit/g cornea).

Hematoxylin and Eosin Staining

Eyeballs of C57BL/6 mice (n = 3/group) harvested at 3 days p.i. were enucleated and embedded in optimum cutting temperature (O.C.T.) compound (Sakura Tissue-Tek, Torrance, CA, USA). After liquid nitrogen froze, eyeballs were sectioned into 9 µm under cryostat and fixed in acetone. Slices were treated by conventional H&E staining and photographed under an optical microscope (Axio Vert; Zeiss, Jena, Germany; at 400× magnification).

Periodic Acid Schiff Staining

Mice eyeballs at 3 days p.i. (n = 3/group) were harvested, embedded, and frozen in O.C.T., and then sectioned by 9 µm under cryostat. Sections were stained with a glycogen PAS staining kit (Leagene, Beijing, China) following the manufacturer's instructions. Each slice was photographed under an optical microscope (Axio Vert; Zeiss, Jena, Germany; at 400× magnification).

Immunofluorescence Staining

The immunofluorescence step refers to the previous study.[21] The mouse eyeballs (n = 3/group) at 3 days p.i. were removed, embedded, and frozen at O.C.T., then sliced into 9 µm-thick tissue sections. After being blocked with goat serum (1:100, Solarbio) for 30 minutes at 37°C, the sections were incubated with anti-NIMP-R14 antibody (1:100; Santa Cruz Biotechnology, Santa, Cruz, CA, USA) at 4°C overnight. Then, slices were stained with FITC-conjugated goat anti-rat (1:50; Elabscience, Wuhan, China) for 1 hour at 37°C. Cell nuclei were stained with 4′, 6-diamidino-2-phenylindole dihydrochloride (DAPI; 1:5; Solarbio). The slides were observed under the fluorescence microscope (Zeiss Axio Vert, Jena, Germany; at 200× magnification).

Real-time PCR

Total RNA of RAW264.7 cells and mouse corneas (n = 5/group) were extracted using the RNAiso Plus reagent (TaKaRa, Dalian, China) and quantified by NanoDrop ND-1000 Spectrophotometry (Thermo Fisher Scientific). RNA samples were reverse transcribed using HiScript III-RT SuperMix-cjj (Vazyme, Nanjing, China) to produce a cDNA template. The procedure of RT-PCR was referred to in previous experimental research.[26] The corresponding primer pair sequences used for RT-PCR are shown in the Table.

Enzyme-Linked Immunosorbent Assay

RAW264.7 cells cultured in 6-well plates were stimulated with inactive *A. fumigatus* hyphae for 1 hour, then treated with 100 µg/mL GA for 23 hours. The supernatant was collected and centrifuged. The ELISA kit (R&D Systems, Minneapolis, MN, USA) was used to detect IL-1β and TNF-α protein levels according to the manufacturer's instructions. The absorbance was measured at 450 nm with a microplate reader.

Western Blot

RAW264.7 cells were lysed in RIPA buffer (Solarbio) containing PMSF (Solarbio) and phosphatase inhibitor (MCE), sonicated, and centrifuged at 12,000 rpm for 5 minutes. BCA kit (Elabscience) was used for protein concentration determination. Total proteins were separated on SDS-PAGE and transferred onto polyvinylidene difluoride (PVDF) membrane (Solarbio). The membranes were blocked in blocking buffer (Solarbio) and incubated with primary antibodies against GADPH (1:2000; Elabscience), HO-1 (1:1000; Abcam), and

Investigative Ophthalmology & Visual Science

Nrf2 (1:1000; Abcam) at 4°C overnight, followed by incubation with goat anti-rabbit secondary antibodies at 37°C for 1.5 hours. Blots were visualized using enhanced chemiluminescence (ECL; Thermo Fisher Scientific, Waltham, MA, USA).

Statistical Analysis

The experimental data were analyzed by GraphPad Prism8.0.2 (GraphPad, San Diego, CA, USA) and expressed by mean ± SEM. The unpaired, two-tailed Student's *t*-test was used to analyze the statistical significance between the two groups. One-way analysis of variance (ANOVA) with Bonferroni's post hoc test was performed to examine the difference among three or more groups. The clinical score in different groups was determined by the Mann-Whitney *U* test. Image J (National Institutes of Health, Bethesda, MD, USA) was used to analyze the images of IFS and Western blot. Any $P < 0.05$ was considered as significant (ns = no significance). All experiments were repeated at least three times to ensure accuracy.

Results

Evaluation of GA Toxicity In Vitro and In Vivo

CCK-8 assay and Draize eye test were performed to determine the toxicity of GA in HCECs and an *A. fumigatus* mouse model, respectively. In HCECs, GA did not affect the cell viability at 100 µg/mL for 48 hours (Fig. 1A). However, GA started inhibiting cell viability at 200 µg/mL (see Fig. 1A), suggesting that GA was cytotoxic to HCECs at 200 µg/mL. In healthy mouse cornea, no pathological or morphological damage was observed in the corneal epithelium of mice treated with 100 µg/mL GA at days 1, 3, and 5 (Fig. 1B). Thus, GA with a concentration of no more than 100 µg/mL was considered safe and applied to the subsequent in vitro and in vivo experiments.

Antifungal Effects of GA In Vitro

We demonstrate that GA has antifungal effects on *A. fumigatus in vitro*. GA started to inhibit *A. fumigatus* growth at 100 µg/mL (Fig. 2A) and markedly inhibited the biofilm formation of *A. fumigatus* starting from 25 µg/mL in a dose-dependent manner (Fig. 2B). H&E staining revealed that the number of *A. fumigatus* conidia adherent to HCECs was significantly reduced in the 100 µg/mL GA-treated group compared with the PBS group (Figs. 2C, 2D). This indicated that GA suppressed *A. fumigatus* adhesion at 100 µg/mL. Moreover, calcofluor white staining and PI staining were performed to evaluate the integrity of the fungal cell wall and membrane. Less fungal cell wall components labeled by calcofluor white were detected in GA-treated *A. fumigatus* than in PBS control (Fig. 2E), suggesting GA disrupted the cell wall integrity. Upon GA treatment, the fluorescent intensity of nuclear and chromosomes exposed from dead fungal cells with impaired membrane was enhanced (Fig. 2F), which also supported that GA may break *A. fumigatus* cell membranes. These findings reveal the antifungal property of GA, which is associated with inhibiting

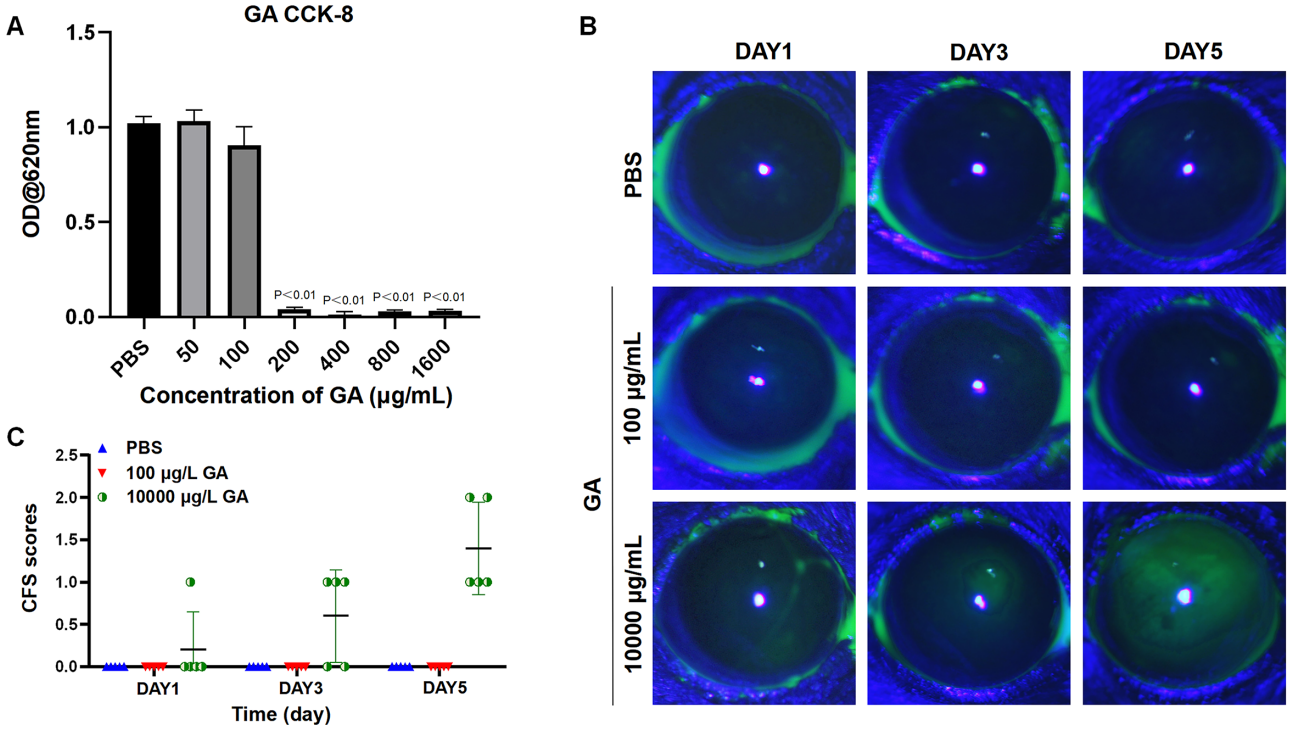

Figure 1. Evaluation of GA toxicity in vitro and in vivo. CCK-8 assay was carried out on HCECs after 48-hour incubation with different concentrations of GA (0, 50, 100, 200, 400, 800, and 1600 µg/mL) (**A**). The Draize eye test was performed on healthy mice ($n = 5$/group/time). Mice corneas were treated with GA at concentrations of 0, 100, and 10000 µg/mL for 5 days, and fluorescein staining was performed at 1, 3, and 5 days post-treatment. Representative light microscopy photographs of fluorescein staining at days 1, 3, and 5 (**B**). All data were mean ± SEM and analyzed by one-way ANOVA with Bonferroni's post hoc test.

Investigative Ophthalmology & Visual Science

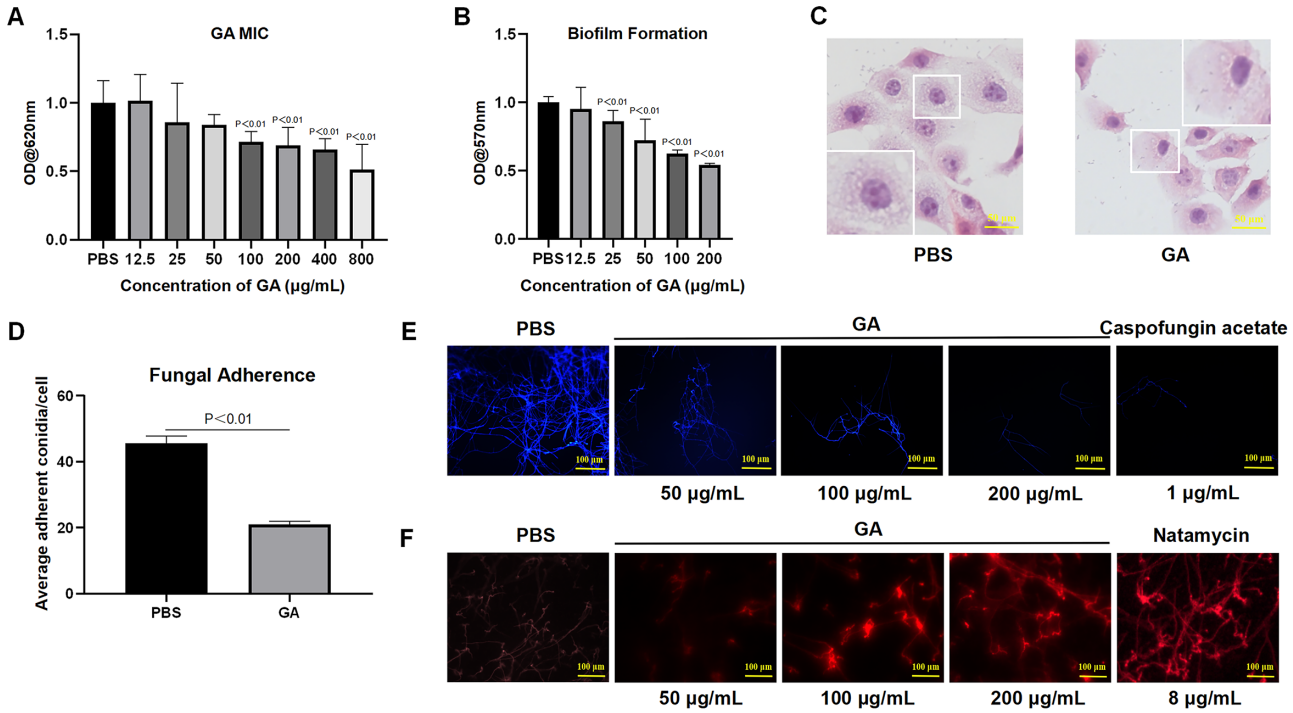

Figure 2. Antifungal effects of GA in vitro. MIC of GA at concentrations of 0, 12.5, 50, 100, 200, 400, and 800 μg/mL for 48 hours in HCECs. GA started to inhibit *A. fumigatus* growth at 100 μg/mL (**A**). Biofilm formation of *A. fumigatus* exposed to different concentrations of GA (0, 12.5, 25, 50, 100, and 200 μg/mL) for 48 hours. GA markedly inhibited biofilm formation of *A. fumigatus* starting from 25 μg/mL in a dose-dependent manner (**B**). H&E staining based fungal adhesion assay showed the number of *A. fumigatus* conidia adherent to HCECs was significantly reduced in the 100 μg/mL GA-treated group compared with PBS control (×400 magnification) (**C**). Quantitative results of H&E staining (**D**). Calcofluor white staining of *A. fumigatus* treated with PBS, Caspofungin acetate (positive control), or different concentrations of GA (50, 100, and 200 μg/mL) for 48 hours in vitro (×20 magnification). GA disrupted the cell wall integrity in a dose-dependent manner (**E**). PI staining of *A. fumigatus* treated with PBS, natamycin (positive control), or different concentrations of GA (50, 100, and 200 μg/mL) for 24 hours in vitro (×20 magnification) (**F**). All data were presented as mean ± SEM. MIC and biofilm formation results were analyzed by one-way ANOVA with Bonferroni's post hoc test, and an unpaired, two-tailed Student's *t*-test was used to compare fungal adhesion results.

biofilm formation and adhesion and disrupting the fungal cell membrane integrity.

GA Improved *A. Fumigatus* Keratitis Outcomes in Mice

To explore the therapeutic effect of GA, 100 μg/mL GA was applied to mice with *A. fumigatus* keratitis, and clinical scores were used to evaluate the severity of keratitis at 1, 3, and 5 days p.i.. Slit-lamp photographs illustrated less ulcer area in GA-treated corneas at 3 and 5 days p.i. compared to PBS control (Fig. 3A). Consistently, GA treatment versus PBS significantly decreased the clinical scores at 3 and 5 days p.i., whereas there was no difference observed at 1-day p.i. (Fig. 3B), indicating that GA could ameliorate the severity of *A. fumigatus* keratitis at 3 and 5 days p.i. However, there was no significant difference in clinical scores between GA and the natamycin group, suggesting that GA treatment had the same therapeutic effects as natamycin. We then examined the fungal load using PAS staining. Fewer hyphae were shown in GA and natamycin-treated corneas compared with the PBS group (Fig. 3C), indicating GA exhibited antifungal activity in *A. fumigatus* keratitis mice with the same ability as natamycin. Furthermore, H&E staining revealed that corneas with 100 μg/mL GA and natamycin treatment were thinner and more organized, with less aggregation of neutrophils and other inflammatory cells in contrast to the PBS group (Fig. 3D). Therefore, we hypothesize that GA may improve *A. fumigatus* keratitis prognosis in mice by inhibiting fungal growth and alleviating the inflammatory response, and the therapeutic effects of GA might be comparable to natamycin.

GA Repressed Neutrophil Infiltration and MPO Activity In Vivo

In order to determine the anti-inflammatory effect of GA, neutrophil infiltration and MPO activity were analyzed in GA-, natamycin-, and PBS-treated mice with *A. fumigatus* keratitis. IFS revealed that 100 μg/mL GA significantly inhibited the infiltration and accumulation of neutrophils in the corneal stroma at 3 days p.i. compared with PBS. This inhibitory impact on neutrophil recruitment was also found in the natamycin-treated group (Figs. 4A, 4B). Similarly, GA- and natamycin- versus PBS-treated mice corneas showed markedly reduced MPO activity at 3 days p.i. (Fig. 4C). These results suggested that GA and natamycin treatment could inhibit neutrophil vitality in *A. fumigatus* keratitis mice.

GA suppressed pro-inflammatory cytokine production and enhanced the expression of Nrf2 and HO-1 in vitro and in vivo. We demonstrate that GA downregulated the expression of pro-inflammatory cytokines in RAW264.7 cells and *A. fumigatus* keratitis mouse models. The inactivated hyphae were used to stimulate RAW264.7 cells for 1 hour, followed

Investigative Ophthalmology & Visual Science

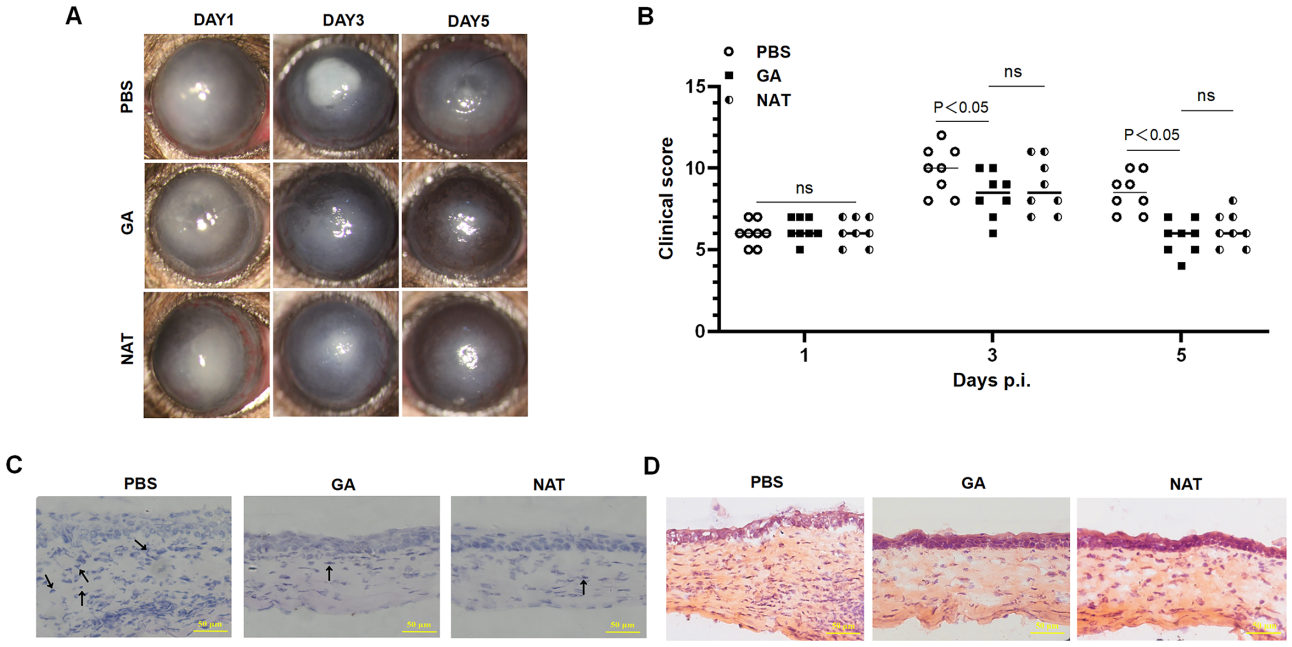

Figure 3. GA improved *A. fumigatus* keratitis outcomes in mice. Representative slit-lamp photographs (**A**) and corresponding clinical scores (**B**) of *A. fumigatus* keratitis mice corneas with PBS, 100 µg/mL GA, and 8 µg/mL natamycin treatment at 1, 3, and 5 days p.i. (n = 8/group/time). PAS staining (for fungal hyphae) (**C**) and H&E staining (**D**) of *A. fumigatus* keratitis mice eyeballs with PBS, 100 µg/mL GA, and 8 µg/mL natamycin treatment at 3 days p.i. (n = 3/group; ×400). The clinical score in different groups was analyzed using the Mann-Whitney U test (ns: no significance).

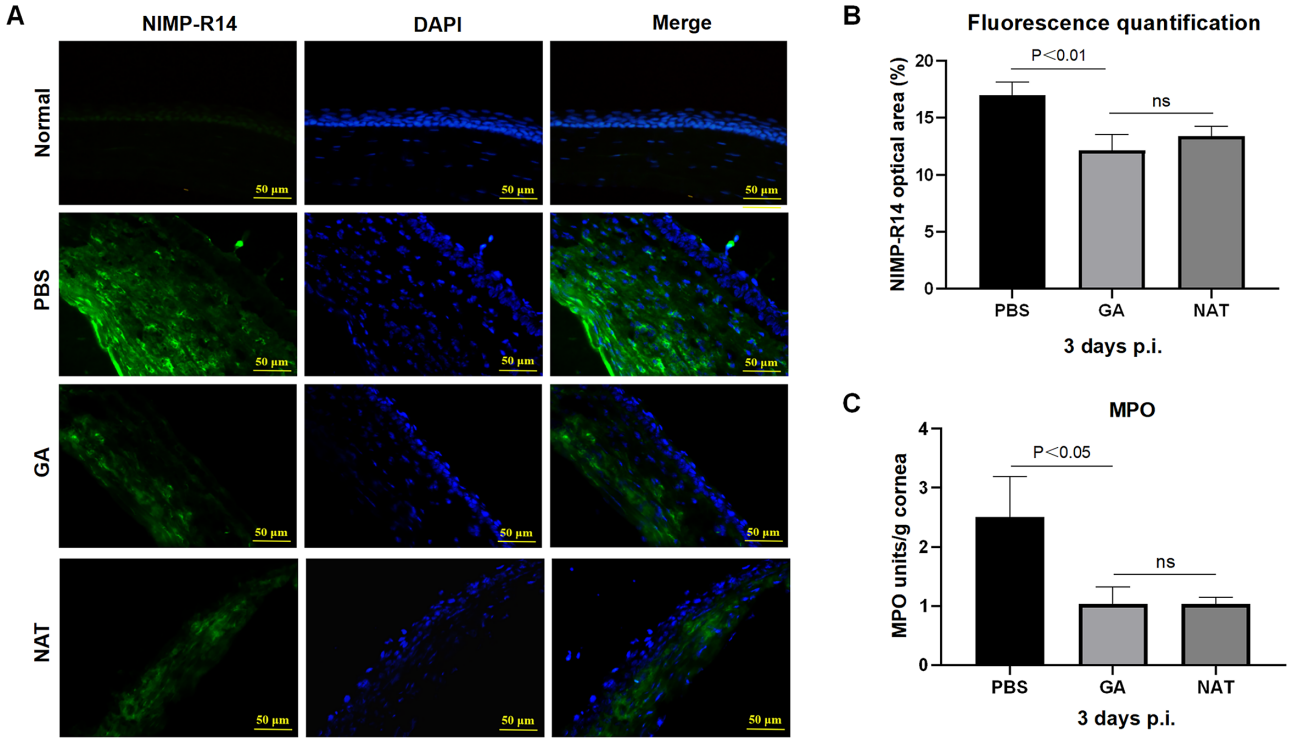

Figure 4. GA repressed neutrophil infiltration and MPO activity in vivo. Representative IFS photographs of *A. fumigatus* keratitis mice corneas treated with PBS, 100 µg/mL GA, and 8 µg/mL natamycin at 3 days p.i. (n = 3/group). *Green*: NIMP-R14 labeled neutrophils; *Blue*: DAPI stained nucleus (×200 magnification) (**A**). IFS quantitative analysis of area fractions of neutrophils (**B**). Quantitative analysis of MPO activity levels of *A. fumigatus* keratitis mice corneas treated with PBS, 100 µg/mL GA, and 8 µg/mL natamycin at 3 days p.i. (n = 5/group) (**C**). All data were mean ± SEM and analyzed by an unpaired, two-tailed Student's t-test.

Investigative Ophthalmology & Visual Science

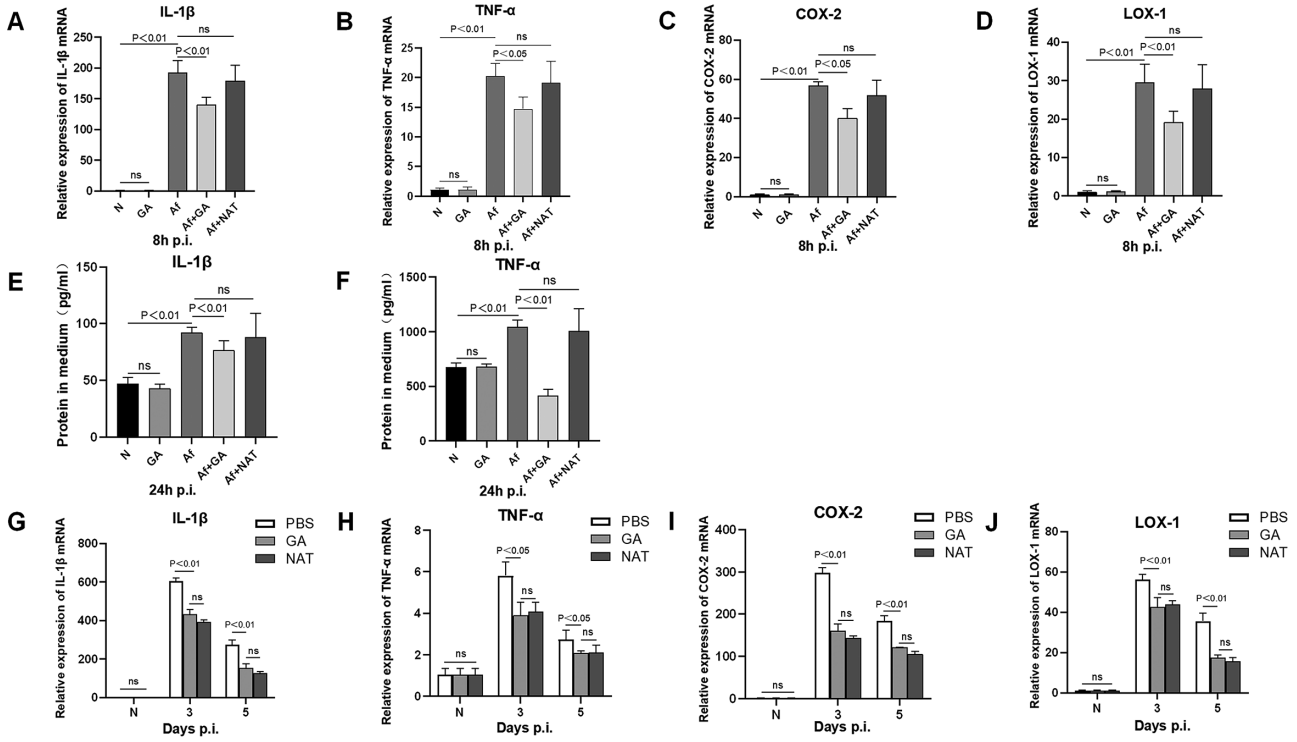

Figure 5. GA suppressed pro-inflammatory cytokine production in RAW264.7 cells and *A. fumigatus* keratitis mouse models. RAW264.7 cells were stimulated with inactivated *A. fumigatus* hyphae for 1 hour and treated with 100 µg/mL GA, 8 µg/mL natamycin, and PBS for 8 hours for RT-PCR and 24 hours for ELISA. RT-PCR results of the mRNA levels of IL-1β (**A**), TNF-α (**B**), COX-2 (**C**), and LOX-1 (**D**), and ELISA results of IL-1β (**E**), TNF-α (**F**) in RAW264.7 cells. In an *A. fumigatus* mouse model, mice corneas were treated with 100 µg/mL GA, 8 µg/mL natamycin, and PBS eye drop 3 times/day, and the mRNA levels of IL-1β (**G**), TNF-α (**H**), COX-2 (**I**), and LOX-1 (**J**) were detected at 3 and 5 days p.i. (n = 6/group/time). All data were mean ± SEM. RT-PCR and ELISA result from RAW264.7 cells were analyzed by one-way ANOVA with Bonferroni's post hoc test. An unpaired, two-tailed Student's *t*-test was used for RT-PCR results from *A. fumigatus* mouse models (N: normal; Af: *A. fumigatus*; ns: no significance).

by 100 µg/mL GA, 8 µg/mL natamycin, and PBS treatment. Both mRNA and protein production of pro-inflammatory factors in RAW264.7 cells was enhanced by *A. fumigatus* treatment (Figs. 5A–F). In comparison with PBS treated group, the mRNA levels of IL-1β (see Fig. 5A), TNF-α (see Fig. 5B), cyclo-oxygenase-2 (COX-2; see Fig. 5C), and lectin-like oxidized low-density lipoprotein receptor-1 (LOX-1; see Fig. 5D) were decreased in GA treated cells at 8 hours post-treatment. Consistently, protein levels of IL-1β (see Fig. 5E), and TNF-α (see Fig. 5F) were reduced in the GA-treated group at 24 hours post-treatment. Whereas in natamycin-treated cells, less reduction was found in the expression of these cytokines but with no statistical significance. In *A. fumigatus* keratitis mouse models, the mRNA expression of IL-1β (Fig. 5G), TNF-α (Fig. 5H), COX-2 (Fig. 5I), and LOX-1 (Fig. 5J) was significantly elevated by *A. fumigatus* infection and markedly repressed by 100 µg/mL GA and 8 µg/mL natamycin versus PBS eye drop treatment at 3 and 5 days p.i. No statistical significance was observed between GA- and natamycin-treated groups. These findings further support our hypothesis that GA could suppress the inflammatory response in RAW264.7 cells and *A. fumigatus* keratitis mouse models. However, natamycin only inhibited the expression of inflammatory mediators in mice with FK, but not in RAW264.7 cells.

Recently, we have described the involvement of the Nrf2/HO-1 signaling pathway in *A. fumigatus* keratitis.[27,28] The activation of Nrf2 signaling plays a protective role throughout the corneal epithelial wound-healing process.[29] HO-1 is one of the downstream target genes of Nrf2.[30] As a cytoprotective anti-inflammatory enzyme, HO-1 is responsible for catalyzing heme degradation.[31] Heme is a known chemoattractant of neutrophils, inducing migration and activation of neutrophils.[30] Therefore, by repressing heme, HO-1 can inhibit the rolling, adhesion, and migration of neutrophils during inflammation.[32] Studies reported that the Nrf2/HO-1 signaling pathway contributes to the anti-inflammatory effects by regulating the recruitment of inflammatory cells.[33,34] Our previous study showed that in *A. fumigatus*-infected corneas, the Nrf2 and HO-1 expression levels were upregulated, suggesting that Nrf2 and HO-1 are involved in the immune process of FK. Thus, to explore the potential mechanisms of GA in anti-inflammation, we detected the effects of GA on the expression of Nrf2 and HO-1 in vitro and in vivo. In RAW264.7 cells stimulated with inactivated *A. fumigatus* hyphae, an 8-hour treatment of 100 µg/mL GA significantly enhanced the mRNA expression of Nrf2 (Fig. 6A) and HO-1 (Fig. 6B) compared with PBS. Consistently, the protein levels of Nrf2 (Figs. 6C, fig66D) and HO-1 (Figs. 6E, 6F) were also increased in GA versus PBS groups. In mice with *A. fumigatus* keratitis, GA treatment improved the mRNA expression of Nrf2 (Fig. 6G), and HO-1 (Fig. 6H) compared to PBS at 3 and 5 days p.i. These results indicated that the anti-inflammatory role of GA could be associated with the Nrf2/HO-1 signaling pathway.

Investigative Ophthalmology & Visual Science

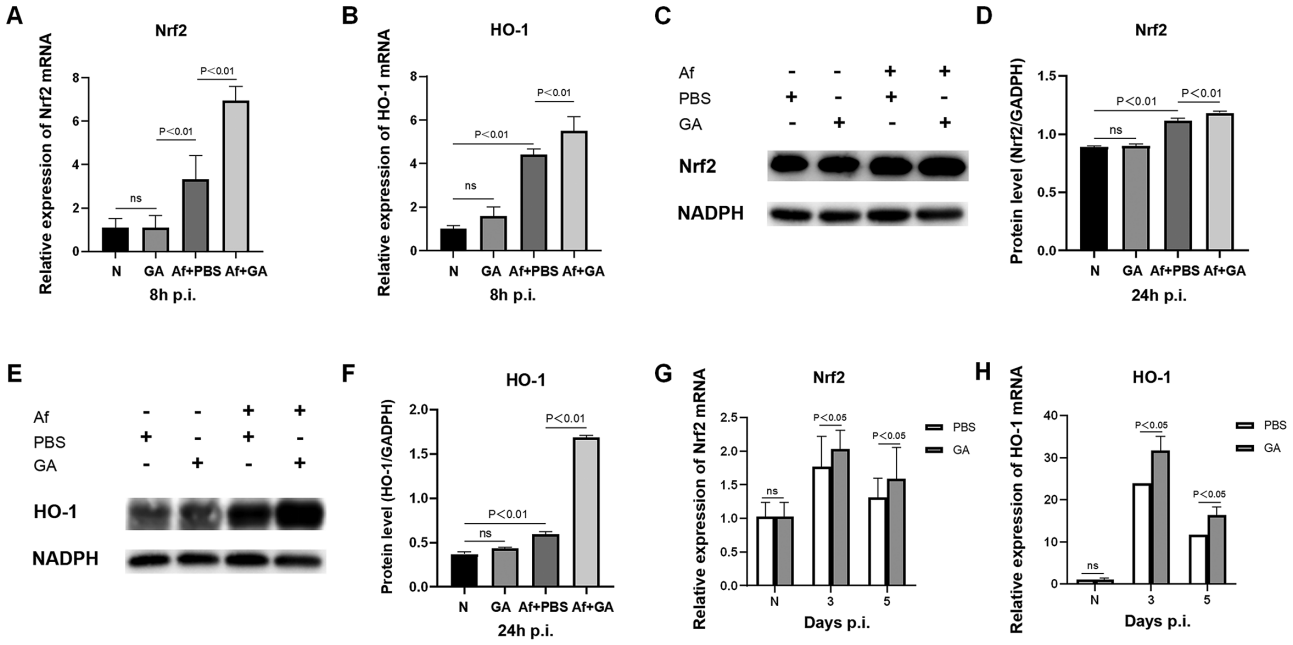

Figure 6. GA enhanced Nrf2 and HO-1 expression in RAW264.7 cells and *A. fumigatus* keratitis mouse models. RAW264.7 cells were stimulated with inactivated *A. fumigatus* hyphae for 1 hour and treated with 100 µg/mL GA or PBS for 8 hours for RT-PCR and 24 hours for Western blot. RT-PCR results of the mRNA levels of Nrf2 (**A**) and HO-1 (**B**) in RAW264.7 cells. Western blot results of Nrf2 (**C**) in RAW264.7 cells and the corresponding quantitative analysis (**D**). Western blot results of HO-1 (**E**) in RAW264.7 cells and the corresponding quantitative analysis (**F**). In an *A. fumigatus* mouse model, mice corneas were treated with 100 µg/mL GA or PBS eye drop 3 times/day, and the mRNA levels of Nrf2 (**G**), HO-1 (**H**) were detected at 3 and 5 days p.i. (n = 6/group/time). All data were mean ± SEM. RT-PCR and Western blot results from RAW264.7 cells were analyzed by one-way ANOVA with Bonferroni's post hoc test. An unpaired, two-tailed Student's t-test was used for RT-PCR results from *A. fumigatus* mouse models (N: normal; Af: *A. fumigatus*; ns: no significance).

Discussion

Our study investigates GA's therapeutic effect on FK in vitro and in the *A. fumigatus* keratitis mouse model. We identified that GA at 100 µg/mL had no cytotoxic effects within 48 hours in HCECs and no corneal toxicity for 5 days of treatment. Thus, we considered that 100 µg/mL GA could be applied as a safe concentration for local corneal therapy.

GA is an abundant phenolic compound in various natural foods.[35] It has a tri-hydroxylated phenolic structure, a benzene ring, a carboxylic grouping, and three hydroxyl groups that endow GA antioxidant properties.[36] Studies showed that GA had an antifungal ability to inhibit fungi sporulation, impede germination of saprobe fungi, and destroy biofilm formation.[37,38] Consistently, we demonstrated that 100 µg/mL GA could repress conidia growth, germination, and biofilm formation of *A. fumigatus*. More importantly, GA reduced the average percentage of adhered conidia adhering to HCECs compared with PBS control, indicating that GA has anti-adhesion capacity. It has been reported that GA could degrade chitin, the major structural component of the phytopathogenic fungi cell walls, by producing the enzyme chitinase.[39] This finding coincides with our staining results, in which 100 µg/mL GA impaired *A. fumigatus* membrane integrity. Besides, GA reduced the activity of CYP51, a key enzyme in the process of fungi ergosterol synthesis.[15] Ergosterol is one of the fungal plasma membrane components, playing a pivotal role in membrane fluidity, permeability, and signal transduction pathways.[40] Thus, we suspect that GA destroys *A. fumigatus* cell membranes and increases membrane permeability by inhibiting the activity of CYP51 enzymes.

In *A. fumigatus* keratitis mice, GA significantly alleviated the severity of FK. PAS staining showed GA obviously decreased the hyphae load in the infected sites, indicating that GA could improve infectious corneal ulcers by limiting the growth of *A. fumigatus*. Similar results were observed in natamycin-treated groups, which suggests that the antifungal effect of GA is comparable to natamycin. On the other hand, the less fungal load is complementary to alleviating inflammatory response and decreasing neutrophil infiltration. Neutrophils are vital inflammatory cells for eliminating intracellular microorganisms.[41] Corneas infected with fungi attract neutrophils released from the limbal vessels to the site of the infection.[42] But the aggregation of neutrophils may result in severe inflammation, which inevitably causes sustained infiltration of inflammatory cells, leading to undesired tissue damage, such as ulceration, cornea perforation, and even vision loss.[43] Earlier studies demonstrated that GA could attenuate neutrophils infiltration and subsequent injury in isoproterenol-induced myocardial infarction.[44] It is in agreement with our results, which showed that 100 µg/mL GA inhibited neutrophils infiltration, alleviated the severity of corneal edema, and made it with more ordered pathological structure in the stroma at 3 days p.i. Clinical scores in GA-treated groups were significantly lower than in PBS-treated groups, and GA-treated corneas were more transparent, with less ulcer area. Therefore, GA markedly contributes to ameliorating corneal damage in *A. fumigatus* keratitis by limiting fungal load and reducing neutrophil recruitment. Interestingly, the natamycin-treated group had a similar therapeutic effect in vivo experiments as GA. Although this therapeutic effect of natamycin could be attributed to its antifungal property, it is still unclear whether natamycin has

a similar anti-inflammatory potential as GA. Thus, in vitro experiments in RAW264.7 cells were conducted to explore the anti-inflammatory activity of GA and natamycin.

During the inflammation process, neutrophils also promote the release of pro-inflammatory chemokines, facilitating the inflammatory response.[45] These released chemokines and cytokines recruit more neutrophils and other immune cells, activating an inflammatory cascade.[46] IL-1β and TNF-α are important pro-inflammatory cytokines involved in the corneal anti-fungal immune response, mainly produced by activated monocytes, mediating acute inflammatory responses.[17] LOX-1 belongs to the C-type lectin family, playing an essential role in the corneal antifungal immune response.[47] COX-2, induced by proinflammatory cytokines, generates prostaglandins, which are supposed to cause inflammation.[48] In our study, the inactivated *A. fumigatus* hyphae were used to stimulate cells. The deactivated fungi have no invasiveness and only stimulate the cells' immune system through residual antigens. We showed that GA treatment decreased *A. fumigatus* stimulated overexpression of IL-1β, TNF-α, LOX-1, and COX-2 in vitro and in vivo, whereas natamycin only decreased them in vivo. This is because natamycin played an antifungal role in the process of *A. fumigatus* keratitis in mice. Less fungal load resulted in less extent of inflammation, thereby reducing the expression of inflammatory cytokines. However, in RAW264.7 cells, natamycin could not reduce the enhanced expression of pro-inflammatory cytokines stimulated by inactivated *A. fumigatus* hyphae, suggesting natamycin has no anti-inflammatory property. Instead, GA showed markedly inflammation-inhibiting activity in vitro.

We have recently described the involvement of the Nrf2/HO-1 signaling pathway in *A. fumigatus* keratitis,[27,28] and GA treatment significantly enhanced *A. fumigatus* induced overexpression of Nrf2 and HO-1 in FK mice models and RAW264.7 cells. These results inspired us that the anti-inflammatory mechanism of GA may be associated with the Nrf2/HO-1 pathways. In the LPS-induced chronic obstructive pulmonary disease (COPD) model, GA treatment resulted in increased protein levels of Nrf2 accompanied by an increment in the transcription of HO-1.[49] Consistently, we observed that the expression of Nrf2 and HO-1 was elevated under the treatment of GA in *A. fumigatus* infected RAW264.7 cells. Although GA induced the enhancement of the Nrf2/HO-1 signaling pathway is validated in FK, the underlying mechanism is still unclear. One possible way besides the transcriptional regulation is that GA might promote the cytonuclear translocation of Nrf2 under inflammatory stress.[50,51] Future studies could focus on how Nrf2/HO-1 is involved in the inflammatory regulation of FK.

In summary, our study investigates the antifungal and anti-inflammatory effects of GA on *A. fumigatus* keratitis in vitro and in vivo. We showed that GA could ameliorate *A. fumigatus* keratitis via inhibiting fungal growth and spore germination, decreasing neutrophils recruitment and infiltration, and increasing the expression of Nrf2 and HO-1, as well as reducing the expression of inflammatory cytokines, such as IL-1β, TNF-α, LOX-1, and COX-2, which suggests that GA could be a potentially effective drug for FK treatment.

Acknowledgments

Supported by the National Natural Science Foundation of China (No. 82101095 and No. 82171029), Youth Project of Natural Science Foundation of Shandong Province (No. ZR2019BH004).

Disclosure: **S. Luan**, None; **X. Peng**, None; **J. Lin**, None; **Y. Zhang**, None; **L. Zhan**, None; **J. Yin**, None; **J. Luan**, None; **X. Ji**, None; **G. Zhao**, None

References

1. Garg P, Roy A, Roy A. Update on fungal keratitis. *Curr Opin Ophthalmol*. 2016;27(4):333–339.
2. Thomas PA, Kaliamurthy J. Mycotic keratitis: epidemiology, diagnosis and management. *Clin Microbiol Infect*. 2013;19:210–220.
3. Gopinathan U, Garg P, Fernandes M, et al. The epidemiological features and laboratory results of fungal keratitis: a 10-year review at a referral eye care center in South India. *Cornea*. 2002;21(6):555–559.
4. Latgé JP. Aspergillus fumigatus and aspergillosis. *Clin Microbiol Rev*. 1999;12(2):310–350.
5. Lakhani P, Patil A, Majumdar S. Challenges in the Polyene- and Azole-Based Pharmacotherapy of Ocular Fungal Infections. *J Ocul Pharmacol Ther*. 2018;35(1):6–22.
6. O'Day DM, Head WS, Robinson RD, et al. Corneal penetration of topical amphotericin B and natamycin. *Curr Eye Res*. 1986;5(11):877–882.
7. O'Day DM, Ray WA, Head WS, et al. Influence of the corneal epithelium on the efficacy of topical antifungal agents. *Invest Ophthalmol Vis Sci*. 1984;V25N7:855–859.
8. Yang K, Zhang L, Liao P, et al. Impact of Gallic Acid on Gut Health: Focus on the Gut Microbiome, Immune Response, and Mechanisms of Action. *Front Immunol*. 2020;9:11:580208.
9. Hargrove TY, Friggeri L, Wawrzak Z, et al. Structural analyses of Candida albicans sterol 14¦Á-demethylase complexed with azole drugs address the molecular basis of azole-mediated inhibition of fungal sterol biosynthesis. *J Biol Chem*. 2017;292:6728–6743.
10. BAN JY, Thuy HT, Lee HJ, et al. Neuroprotective properties of gallic acid from Sanguisorbae radix on amyloid beta protein (25—35)-induced toxicity in cultured rat cortical neurons. *Biol. Pharm. Bull*. 2008;31:149–153.
11. You BR, Kim SZ, Kim SH. Gallic acid-induced lung cancer cell death is accompanied by ROS increase and glutathione depletion. *Mol Cell Biochem*. 2011;357:295–303.
12. Hsieh SC, Chi-Hao W, Chun-Chi W, et al. Gallic acid selectively induces the necrosis of activated hepatic stellate cells via a calcium-dependent calpain I activation pathway. *Life Sciences*. 2014;102:55–64.
13. Zhu L, Gu PQ, Shen H.Gallic acid improved inflammation via NF-κB pathway in TNBS-induced ulcerative colitis. *Int Immunopharmacol*. 2019;67:129–137.
14. Zhi-Jian L, Meng L, Dawuti G, et al. Antifungal Activity of Gallic Acid In Vitro and In Vivo. *Phytother Res*. 2017;31:1039–1045.
15. Richter RK, Mickus DE, Rychnovskyc SD, et al. Differential modulation of the antifungal activity of amphotericin B by natural and ent-cholesterol. *Bioorg Med Chem Lett*. 2004;14:115–118.
16. Sony P, Kalyani M, Jeyakumari D, et al. In vitro antifungal activity of cassia fistula extracts against fluconazole resistant strains of Candida species from HIV patients. *J Mycol Med*. 2018;28:193–200.
17. Yang H, Wang Q, Han L, et al. Nerolidol inhibits the LOX-1 /IL-1β signaling to protect against the Aspergillus fumigatus keratitis inflammation damage to the cornea. *Int Immunopharmacol*. 2020;80:106118.
18. Liu YL, Hsu CC, Huang HJ, et al. Gallic Acid Attenuated LPS-Induced Neuroinflammation: Protein Aggregation and Necroptosis. *Mol Neurobiol*. 2020;57:96–104.

Investigative Ophthalmology & Visual Science

19. Zhoua D, Yanga Q, Tian T, et al. Gastroprotective effect of gallic acid against ethanol-induced gastric ulcer in rats: Involvement of the Nrf2/HO-1 signaling and anti-apoptosis role. *Biomed Pharmacother*. 2020;126:110075.
20. Tang Q, Che CY, Lin J, et al. Maresin1 regulates neutrophil recruitment and IL-10 expression in Aspergillus fumigatus keratitis. *Int Immunopharmacol*. 2019;69:103–108.
21. Yin J, Peng XD, Lin J, et al. Quercetin ameliorates Aspergillus fumigatus keratitis by inhibiting fungal growth, toll-like receptors and inflammatory cytokines. *Int Immunopharmacol*. 2021;93:107435.
22. Zhan L, Peng XD, Lin J, et al. Honokiol Reduces Fungal Load, Toll-Like Receptor-2, and Inflammatory Cytokines in Aspergillus fumigatus Keratitis. *Invest Ophthalmol Vis Sci*. 2020;61:48.
23. Zhu Y, Peng X, Zhang Y, et al. Baicalein Protects Against Aspergillus fumigatus Keratitis by Reducing Fungal Load and Inhibiting TSLP-Induced Inflammatory Response. *Invest Ophthalmol Vis Sci*. 2021;62(6):26.
24. BenSaad LA, Kim KH, Quah CC, et al. Anti-inflammatory potential of ellagic acid, gallic acid and punicalagin A&B isolated from Punica granatum. *BMC Complement Altern Med*. 2017;17:47.
25. Yin M, Li C, Peng XD, et al. Expression and role of calcitonin gene-related peptide in mouse Aspergillus fumigatus keratitis. *Int J Ophthalmol*. 2019;12:697–704.
26. Peng XD, Zhao GQ, Lin J, et al. Interaction of mannose binding lectin and other pattern recognition receptors in human corneal epithelial cells during Aspergillus fumigatus infection. *Int Immunopharmacol*. 2018;63:161–169.
27. Fan YQ, Li C, Peng XD, et al. Perillaldehyde Ameliorates Aspergillus fumigatus Keratitis by Activating the Nrf2/HO-1 Signaling Path way and Inhibiting Dectin-1-Mediated Inflammation. *Invest Ophthalmol Vis Sci*. 2020;61:51.
28. Gu LW, Lin J, Wang Q, et al. Dimethyl itaconate protects against fungal keratitis by activating the Nrf2/HO-1 signaling Pathway. *Immunol Cell Biol*. 2020;98:229–241.
29. Hayashi R, Himori N, Taguchi K, et al. The role of the Nrf2-mediated defense system in corneal epithelial wound healing. *Free Radic Biol Med*. 2013;61:333–342.
30. Choi A.M., Alam J. Heme oxygenase-1: function, regulation, and implication of a novel stress-inducible protein in oxidant-induced lung injury. *Am J Respir Cell Mol Biol*. 1996;15:9–19.
31. Patil K, Bellner L, Cullaro G, et al. Heme oxygenase-1 induction attenuates corneal inflammation and accelerates wound healing after epithelial injury. *Invest Ophthalmol Vis Sci*. 2008;49:3379–3386.
32. Freitas A, Alves-Filho JC, Secco DD, et al. Heme oxygenase/carbon monoxide-biliverdin pathway down regulates neutrophil rolling, adhesion and migration in acute inflammation. *Br J Pharmacol*. 2006;149:345–354.
33. Mills EL, Ryan DG, Prag HA, et al. Itaconate is an anti-inflammatory metabolite that activates Nrf2 via alkylation of KEAP1. *Nature*. 2018;556:113–117.
34. Kundu JK, Surh YJ. Nrf2-Keap1 signaling as a potential target for chemoprevention of inflammation-associated carcinogenesis. *Pharm Res*. 2010;27:999–1013.
35. Bravo L. Polyphenols: chemistry, dietary sources, metabolism, and nutritional significance. *Nutr Rev*. 1998;56:317–333.
36. Pannala AS, Chan TS, O'Brien PJ, et al. Flavonoid B-ring chemistry and antioxidant activity: fast reaction kinetics. *Biochem Biophys Res Commun*. 2001;282:1161–1168.
37. Lima VN, Oliveira-Tintino DM, Santos ES, et al. Antimicrobial and enhancement of the antibiotic activity by phenolic compounds: Gallic acid, caffeic acid and pyrogallol. *Microb Pathog*. 2016;99:56–61.
38. Alves CT, Ferreira IC, Barros L, et al. Antifungal activity of phenolic compounds identified in flowers from North Eastern Portugal against Candida species. *Future Microbiol*. 2014;9:139–146.
39. Nguyen D, Seo D, Lee H, et al. Antifungal activity of gallic acid purified from Terminalia nigrovenulosa bark against Fusarium solani. *Microb Pathog*. 2013;56:8–15.
40. Yang JY, Liao MJ, Yang L,, et al. Advances in sterol 14alpha-demethylase (CYP51). *Sheng Wu Gong Cheng Xue Bao*. 2008;24:1681–1688.
41. Desai JV, Lionakis MS. The role of neutrophils in host defense against invasive fungal infections. *Curr Clin Microbiol Rep*. 2018;5:181–189.
42. Silva MT, Correia-Neves M. Neutrophils and macrophages: the main partners of phagocyte cell systems. *Front Immunol*. 2012;3:174.
43. Wu J, Zhang WS, Zhao J, et al. Review of clinical and basic approaches of fungal keratitis. *Int J Ophthalmol*. 2016;9:1676–1683.
44. Cheng YY, Zhao J, Tse HF, et al. Plant Natural Products Calycosin and Gallic Acid Synergistically Attenuate Neutrophil Infiltration and Subsequent Injury in Isoproterenol-Induced Myocardial Infarction: A Possible Role for Leukotriene B4 12-Hydroxydehydrogenase? *Oxid Med Cell Longev*. 2015;2015:434052.
45. Amulic B, Cazalet C, Hayes GL, et al. Neutrophil function: from mechanisms to disease. *Annu Rev Immunol*. 2012;30:459–489.
46. Nguyen-Ngo C, Salomon C, Lai A, et al. Anti-inflammatory effects of gallic acid in human gestational tissues in vitro. *Reproduction*. 2020;160:561–578.
47. He K, Yue LH, Zhao GQ, et al. The role of LOX-1 on innate immunity against Aspergillus keratitis in mice. *Int J Ophthalmol*. 2016;9:1245–1250.
48. Gilroy DW, Colville-Nash PR. New insights into the role of COX 2 in inflammation. *J Mol Med (Berl)*. 2000;78(3):121–129.
49. Singla E, Puri G, Dharwal V, et al. Gallic acid ameliorates COPD-associated exacerbation in mice. *Mol Cell Biochem*. 2021;476:293–302.
50. Hua L, Yan-Hua X, Qian Y, et al. Cardioprotective effect of paeonol and danshensu combination on isoproterenol-induced myocardial injury in rats. *PLoS One*. 2012;7(11):e48872.
51. Xu X, Li H, Hou X, et al. Punicalagin Induces Nrf2/HO-1 Expression via Upregulation of PI3K/AKT Pathway and Inhibits LPS-Induced Oxidative Stress in RAW264.7 Macrophages. *Mediators Inflamm*. 2015;2015:380218.

Investigative Ophthalmology & Visual Science